

# Journal of Nanophotonics

Nanophotonics.SPIEDigitalLibrary.org

## Effect of annealing InGaP/InAlGaP laser structure at 950°C on laser characteristics

Ahmad A. Al-Jabr  
Pawan Mishra  
Mohammed A. Majid  
Tien Khee Ng  
Boon S. Ooi

**SPIE.**

Ahmad A. Al-Jabr, Pawan Mishra, Mohammed A. Majid, Tien Khee Ng, Boon S. Ooi, "Effect of annealing InGaP/InAlGaP laser structure at 950°C on laser characteristics," *J. Nanophoton.* **10**(3), 036004 (2018), doi: 10.1117/1.JNP.10.036004.

# Effect of annealing InGaP/InAlGaP laser structure at 950°C on laser characteristics

Ahmad A. Al-Jabr,<sup>a</sup> Pawan Mishra,<sup>a</sup> Mohammed A. Majid,<sup>a,b</sup>  
Tien Khee Ng,<sup>a</sup> and Boon S. Ooi<sup>a,\*</sup>

<sup>a</sup>King Abdullah University of Science & Technology, Photonics Laboratory,  
Thuwal 23955-6900, Saudi Arabia

<sup>b</sup>Effat University, Electrical and Computer Engineering Department, Jeddah, Saudi Arabia

**Abstract.** We achieved considerable laser diode (LD) improvement after annealing InGaP/InAlGaP laser structure at 950°C for a total annealing time of 2 min. The photoluminescence intensity is increased by 10 folds and full-wave at half-maximum is reduced from ~30 to 20 nm. The measured LDs exhibited significantly reduced threshold current ( $I_{th}$ ), from 2 to 1.5 A for a 1-mm long LD, improved internal efficiency ( $\eta_i$ ), from 63% to 68%, and increased internal losses  $\alpha_i$ , from 14.3 to 18.6 cm<sup>-1</sup>. Our work suggests that the use of strain-induced quantum well intermixing is a viable solution for high-efficiency AlGaInP devices at shorter wavelengths. The advent of laser-based solid-state lighting (SSL) and visible-light communications (VLC) highlighted the importance of the current findings, which are aimed at improving color quality and photodetector received power in SSL and VLC, respectively, via annealed red LDs. © The Authors. Published by SPIE under a Creative Commons Attribution 3.0 Unported License. Distribution or reproduction of this work in whole or in part requires full attribution of the original publication, including its DOI. [DOI: [10.1117/1.JNP.10.036004](https://doi.org/10.1117/1.JNP.10.036004)]

**Keywords:** AlGaInP; semiconductor laser; quantum well intermixing; internal efficiency.

Paper 16066 received Apr. 19, 2016; accepted for publication Jul. 6, 2016; published online Jul. 28, 2016.

## 1 Introduction

Red laser diodes (LDs) emitting in the range of 630 to 690 nm are constructed from InGaP/InAlGaP laser structures. In addition to their conventional applications in compact data storage and pointing devices, these LDs have important applications in commercial laser projector TVs, laser-based solid-state lighting (SSL), and spectral-efficient visible-light communications (VLC). Related to SSL and VLC, Janjua et al.<sup>1</sup> recently achieved simultaneous implementation of 4.8 Gbps (gigabits per second) VLC and daylight illumination in which data were encoded into the red LD, and the continuous-wave (CW) blue- and green-LDs served as the other two primary colors for white light generation. An incremental intensity ratio of blue(B)–green(G)–red(R) was required to achieve a reasonable correlated color temperature (CCT) and color rendering index ( $R_a$ ). Therefore, increasing the red LD intensities would be the best approach to maximize the received power at the detector end in VLC.<sup>1</sup> Moreover, blueshifting the wavelength of the red LD increases the perceived brightness in human photopic vision and will, therefore, lead to higher overall luminous brightness of the eventual RGB-laser light bulbs or projectors.

Despite the need for high-power and shorter wavelength red LDs, a reduction in the wavelength below 630 nm by typical growth methods, such as metal-organic chemical vapor deposition (MOCVD) or molecular beam epitaxy (MBE), is extremely difficult to achieve. If aluminum-free active layers (In<sub>x</sub>Ga<sub>1-x</sub>P layers) are used in the growth, then there is a limited window in which the mole fraction  $x$  can be varied while keeping the layer matched to the GaAs substrate.<sup>2</sup> In contrast, aluminum-rich [In<sub>y</sub>(Al<sub>x</sub>Ga<sub>1-x</sub>)<sub>1-y</sub>P] active layers can be used to grow active layers. Increasing the Al content is the ideal solution because the lattice constant of

\*Address all correspondence to: Boon S. Ooi, E-mail: [boon.ooi@kaust.edu.sa](mailto:boon.ooi@kaust.edu.sa)

the quaternary will hardly change. However, increasing the Al content  $x$  to more than 0.1 severely reduces the optical efficiency of the material due to oxygen-related deep-level defects and increases the threshold current of LDs.<sup>3-5</sup>

The reason for this low efficiency is that Al is a reactive element that oxidizes even in a very-high vacuum and high-temperature growth environment. Therefore, increasing the Al content during growth to create efficient devices is the primary obstacle to producing efficient LEDs and LDs with Al-rich active layers. These factors constitute a major obstacle in the production of LDs emitting below 630 nm.<sup>6</sup>

Recently, we developed a quantum well intermixing technique<sup>7</sup> that enables a further increase in Al content in the active layer. We achieved lasing in the orange (608 nm) at room temperature (RT).<sup>8</sup> Using this technique, we were able to further blueshift the emission from 635 to 565 nm. However, as the laser structure is intermixed, more point defects are introduced into the laser structure, reducing the output power and the performance of the intermixed devices. Consequently, we have lower output power at yellow emission.<sup>8</sup>

There were a number of investigations of the effect of annealing on the performance of the InGaP/InAlGaP laser structure. One of the main concerns when annealing InGaP/InAlGaP laser structure is the integrity of the top surface. Annealing at high temperatures causes the top surface to roughen. Therefore, a layer of dielectric film is needed to protect the surface. Floyd et al. performed annealing after capping the top surface by SiO<sub>2</sub> film deposited using plasma-enhanced chemical vapor deposition, and limited the annealing temperature to 400°C, and obtained an improvement in threshold current  $I_{th}$ , from 20 to 18 mA.<sup>9</sup> A similar procedure was performed; the annealing temperature was set to 450°C for 30 min. Improvement in the threshold current was observed for ridge lasers from 33 to 25 mA.<sup>10</sup> Dekker et al. increased the temperature to 875°C for 1 s<sup>11</sup> without device demonstration. Improvements are illustrated by the improved carrier lifetimes from time-resolved PL measurements and the reduction of deep-level traps by deep-level trap spectroscopy. In this work, we annealed at a relatively elevated temperature of 950°C for a relatively longer time, 2 min, and applied a relatively thick film of SiO<sub>2</sub> 1.5  $\mu$ m. We studied the effect of annealing on PL peak, PL intensity, the threshold current ( $I_{th}$ ), internal efficiency  $\eta_i$ , and optical losses  $\langle\alpha_i\rangle$ .

## 2 Experiment

A single quantum well (SQW) InGaP/InAlGaP laser structure was grown on a 10 deg offcut GaAs substrate using MOCVD, as shown in Fig. 1. The structure consisted of a 200-nm, Si-doped, GaAs buffer layer with a carrier concentration of 1 to 2  $\times 10^{18}$  cm<sup>-3</sup>, a 1- $\mu$ m-thick

[200 nm]	p-GaAs $2 \times 10^{19}$
[75 nm]	p-In <sub>0.5</sub> Ga <sub>0.5</sub> P $3 \times 10^{18}$
[1000 nm]	p-In <sub>0.5</sub> Al <sub>0.5</sub> P $1 \times 10^{18}$
[80 nm]	In <sub>0.5</sub> Al <sub>0.3</sub> Ga <sub>0.2</sub> P barrier
[6 nm]	In <sub>0.47</sub> Ga <sub>0.53</sub> P QW
[80 nm]	In <sub>0.5</sub> Al <sub>0.3</sub> Ga <sub>0.2</sub> P barrier
[1000 nm]	n-In <sub>0.5</sub> Ga <sub>0.5</sub> P $1 \times 10^{18}$
[200 nm]	n-GaAs $2 \times 10^{18}$
n-GaAs substrate	GaAs substrate

**Fig. 1** A single QW InGaP/InAlGaP laser structure grown using MOCVD.

n-In<sub>0.5</sub>Al<sub>0.5</sub>P lattice-matched lower cladding layer with a carrier concentration of  $1 \times 10^{18} \text{ cm}^{-3}$ , a 6-nm-thick InGaP SQW layer sandwiched between two 80-nm undoped In<sub>0.5</sub>Al<sub>0.3</sub>Ga<sub>0.2</sub>P waveguide layers, a 1- $\mu\text{m}$ -thick Zn-doped In<sub>0.5</sub>Al<sub>0.5</sub>P lattice-matched upper cladding layer with a carrier concentration of  $1 \times 10^{18} \text{ cm}^{-3}$ , a 75-nm lattice-matched p-In<sub>0.5</sub>Ga<sub>0.5</sub>P barrier reduction layer with a carrier concentration of  $3 \times 10^{18} \text{ cm}^{-3}$ , and a 200-nm highly doped p-GaAs contact layer with a carrier concentration of  $2$  to  $3 \times 10^{19} \text{ cm}^{-3}$ . The laser was designed to have a peak emission at  $635 \pm 3 \text{ nm}$ .

The laser sample was cleaved to  $\sim 1 \times 1 \text{ cm}$ . The sample was cleaned, and a 1- $\mu\text{m}$  film of SiO<sub>2</sub> was deposited. The samples were annealed using rapid thermal processing at 950°C for 30 s after placing the sample between two fresh GaAs pieces to keep the As overpressure as described in Refs. 12 and 13. The process was repeated four times. SiO<sub>2</sub> film then was removed through dry etching. The surface morphology of samples before and after annealing was characterized using atomic force microscopy (AFM). The changes induced by the above procedure were measured at RT using PL spectroscopy equipped with a 473-nm cobalt laser as the excitation source. The PL of the sample was measured after the process. Laser devices were fabricated from the annealed sample and an as-grown laser sample to make broad area lasers with 75  $\mu\text{m}$  stripes. Laser devices of different cavity lengths were cleaved and characterized at RT.

### 3 Results and Discussion

The rapid thermal annealing process at a temperature of 950°C, or above the epitaxy growth temperature for an extended period of up to 2 min, has been widely implemented as optimum annealing conditions to out-annealed grown-in defects.<sup>13–16</sup> To minimize group-V outdiffusion that will increase surface roughness, and group-III vacancy generation that will result in a large degree of quantum-well intermixing, four cycles annealing at 950°C for 30 s each was performed. The focus in this paper is on the performance of LD after a low degree of intermixing, limited to 5-nm blueshift. A different batch of laser wafers was used from the one used earlier in Ref. 7, and therefore, further optimization was performed for the devices used herein. To minimize As outdiffusion, the annealing was performed with the laser sample sandwiched between two fresh GaAs pieces. This procedure provides the As over-pressure during annealing. Figure 2(a) shows the AFM image, which depicts the surface morphology of the as-grown sample, with root-mean-square (RMS) roughness of 2.65 nm. Postgrowth annealing and removal of the SiO<sub>2</sub> layer resulted in the increase of RMS surface roughness to 4.62 nm, as shown in Fig. 2(b).

Figure 3 shows the PL of the sample before and after intermixing. The intensity of the PL signal was enhanced  $\sim 10$  folds, from 70 to 735 counts and the full-wave at half-maximum (FWHM) was reduced from  $\sim 30$  to 20 nm. The strong PL signal, the narrow FWHM, and the good surface morphology after the intermixing process suggest that the fabricated devices were comparable to as-grown lasers. The as-grown QW emitted at 641 nm (shown in Fig. 3). The blueshift of  $\tilde{6} \text{ nm}$  (15 meV) is due to the interdiffusion of Al and Ga atoms between the QW and the barriers. The reduction in FWHM can be related to the removal of oxygen-related defects as in Ref. 11. Here, we are using a similar design to our previously reported intermixing process,<sup>7</sup> but with different growth. Therefore, the blueshift is lower than previously reported.

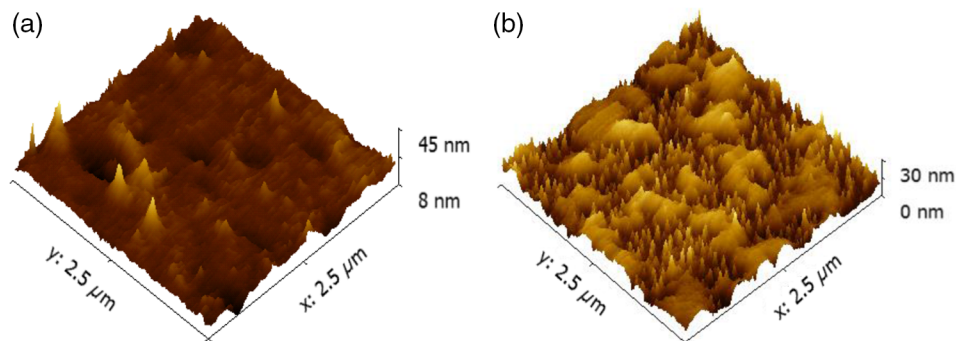


**Fig. 2** The AFM images for InGaP/InAlGaP LDs: (a) the as-grown surface and (b) the surface after annealing and removal of SiO<sub>2</sub> film.

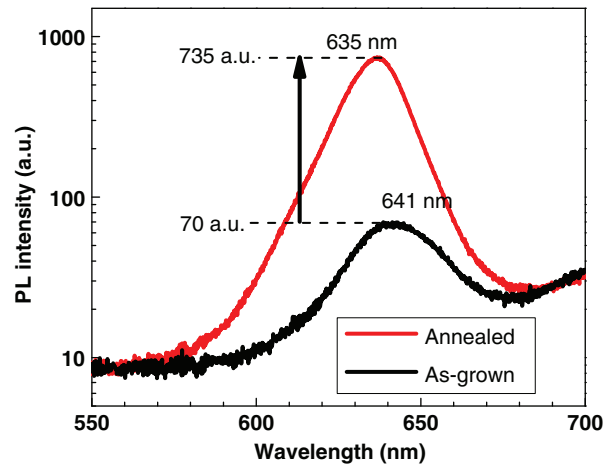


**Fig. 3** The PL signal of the annealed laser structure compared to the as-grown PL signal. Annealed sample emissions are blueshifted by  $\sim 6$  nm with an increase in the PL intensity (10 folds) and a reduction in the FWHM by  $\sim 10$  nm.

As-grown and annealed samples were fabricated in the same manner. Figure 4 shows the lasing spectrum of the fabricated devices with a 1-mm length. The devices were pumped at a  $1.1I_{th}$ , and the lasing spectrum was measured by placing an optical fiber close to the laser facets. The as-grown laser devices emitted at 644 nm, whereas the lasing wavelength of the annealed devices was  $\sim 638$  nm. The small redshift between the measured PL and electroluminescence (EL) of both the annealed and as-grown devices at peak emission is due to heating.

Next, we cleaved the as-grown and annealed laser samples to lengths of 0.4, 0.6, and 0.8 mm and measured the thresholds of multiple devices at each length. Figure 5 shows the threshold current of the annealed devices compared to the as-grown devices. The threshold current  $I_{th}$  of the annealed laser with a length of 1 mm is 1.5 A, whereas the as-grown laser has a threshold current of 2 A, which is  $\sim 25\%$  lower. As the length of the devices is reduced, the threshold current difference between the annealed and as-grown devices becomes smaller. The slope efficiency of the annealed devices is lower than that of the as-grown devices.

Figure 6 shows  $LI$  and  $IV$  curves at high-current pumping for 0.4- and 1-mm devices. The roll over for the annealed devices with respect to the as-grown device samples is faster, and the turn-on voltage is higher. We believe that the increase in the series resistance is due to annealing at elevated temperature, which causes As and dopants to diffuse out of the contact layer.

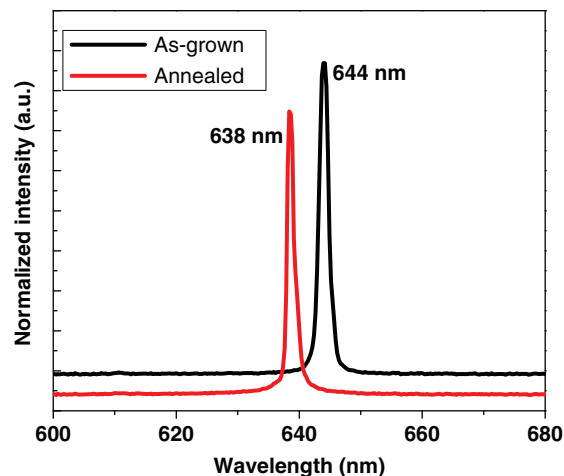


**Fig. 4** The EL of as-grown and annealed devices cleaved to 1-mm long devices. The as-grown and annealed devices have lasing peaks at 644 and 638 nm, respectively.

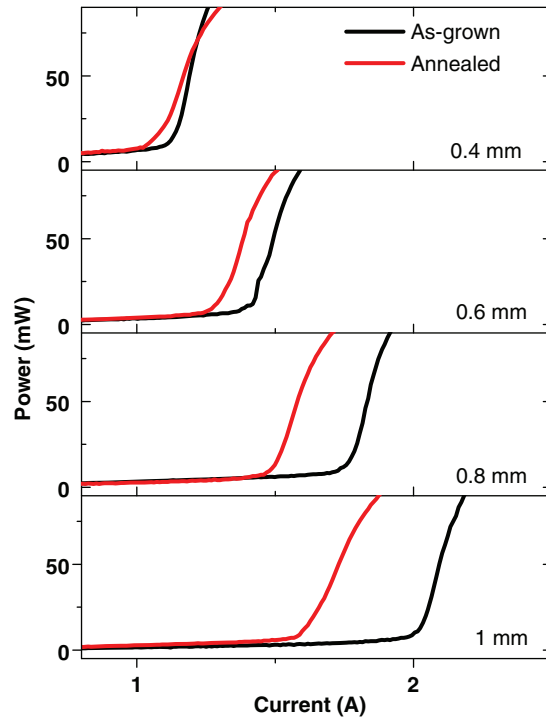


**Fig. 5** Threshold currents of as-grown devices compared to annealed devices of different device lengths. Annealed devices have lower threshold currents and lower differential efficiencies. For longer devices, the differences are clearer.

To determine the internal optical loss  $\langle \alpha_i \rangle$  and the internal quantum efficiency (IQE, or  $\eta_i$ ), of the fabricated devices, we followed the standard procedure in Ref. 17 and plotted the inverse differential quantum efficiency ( $1/\eta_d$ ) against the device length  $L$  in Fig. 7. The quantum efficiency  $\eta_i$  of the annealed devices is 68%, which is better than that of the as-grown devices. However, the internal optical loss increased from 14.3 to 18.6  $\text{cm}^{-1}$ . The annealed devices have a rougher surface and higher resistance compared to that of the as-grown sample, leading to the increase in turn-on resistance, and hence a reduction in slope efficiency. On the other hand, the higher IQE is due to the out-annealing of grown-in defects.

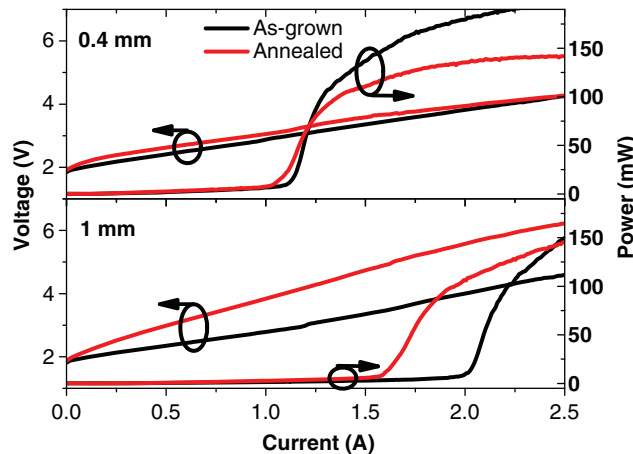


**Fig. 6**  $LI$  and  $IV$  curves of the annealed and as-grown laser devices with 0.4-and 1-mm lengths. The rolling over of the annealed devices is faster, and the series resistance is higher.

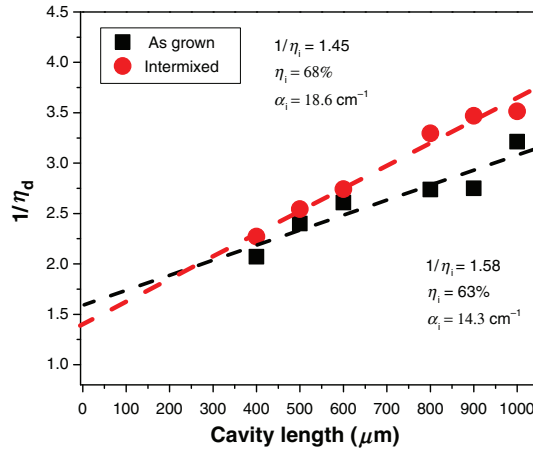


Fig. 7 A plot of the inverse differential quantum efficiency versus the laser cavity length.

Figure 8 shows a plot of the threshold current density of the annealed and as-grown laser devices versus the inverse length. The transparency current ( $J_{th0}$ ) for the as-grown devices is 1850 A/cm<sup>2</sup>, while it is 1100 A/cm<sup>2</sup> for the annealed devices.

In this process on the InGaP/InAlGaP material system, annealing has improved the performance of the laser devices. Adding the results we achieved before from orange and yellow devices,<sup>8,18,19</sup> the results can be explained if we split the process into three subprocesses. The first subprocess is the creation of defects. These defects are created at the interface of the capping dielectric-laser interface and propagate throughout the laser structure. The point defects are created due to the difference in expansion coefficients.<sup>20</sup> Defects, created during annealing, increase the nonradiative recombination centers and the optical losses for light propagation inside the structure. Such effects have already been discussed in Ref. 21. We believe the defects created during the annealing process are responsible for the increase in  $\alpha_i$  in the annealed devices. The amount of defects can be controlled by reducing the annealing time or reducing the applied strain from the dielectric film. The second subprocess is the interdiffusion of group-III atoms between the QW and the barriers. As a result, the bandgap of the QW is blueshifted as more Al atoms diffuse into the QW. As the temperature and time are increased, the amount of diffusion increases. These two subprocesses are well known in the literature and expected.<sup>22</sup> We have experienced similar effects when applying a large degree of intermixing.<sup>8,18</sup> The third subprocess, which we are emphasizing, is the reduction of deep-level traps. The considerable improvement in PL intensity and reduction in FWHM with the enhancement in the threshold current  $J_{th}$  can be related to the reduction in deep-level traps and oxygen-related defects due to the elevated temperature as explained in Ref. 9. However, the improvement we are getting in this work is higher than reported.

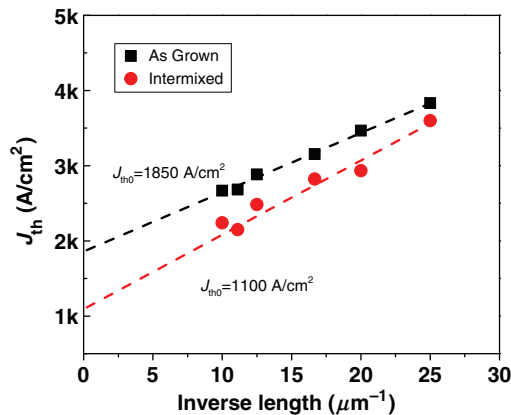


Fig. 8 Threshold current density  $J_{th}$  versus the inverse cavity length  $1/L$ .

## 4 Conclusion

In this work, we performed annealing on the InGaP/InAlGaP laser structure, and obtained considerable improvement in the PL intensity, and internal quantum efficiency, as well as a reduction in the threshold current of the laser. We related this improvement to the out-annealing of the oxygen-related defects. A small reduction in wavelength is due to the interdiffusion of Al atoms from the quantum barrier to QW. This technique represents a solution to achieve high-efficiency InAlGaP devices at the shorter wavelengths of yellow and orange.

## Acknowledgments

This work was supported by King Abdullah University of Science and Technology (KAUST) under Baseline Funding (BAS/1/1614-01-01) and Competitive Research Grant (CRG-1-2012-OOI-010).

## References

1. B. Janjua et al., "Going beyond 4 Gbps data rate by employing RGB laser diodes for visible light communication," *Opt. Express* **23**, 18746–18753 (2015).
2. L. McGill, J. Wu, and E. Fitzgerald, "Yellow-green emission for ETS-LEDs and lasers based on a strained-InGaP quantum well heterostructure grown on a transparent, compositionally graded AlInGaP buffer," in *MRS Proc.*, p. M7. 5 (2002).
3. M. Suzuki et al., "Reduction of residual oxygen incorporation and deep levels by substrate misorientation in InGaAlP alloys," *J. Cryst. Growth* **133**, 303–308 (1993).
4. S. Naritsuka et al., "Photoluminescence studies on InGaAlP layers grown by low-pressure metalorganic chemical vapor deposition," *J. Electron. Mater.* **20**, 687–690 (1991).
5. P. Altieri et al., "Internal quantum efficiency of high-brightness AlGaInP light-emitting devices," *J. Appl. Phys.* **98**, 086101 (2005).
6. G. B. Stringfellow and M. G. Craford, *High Brightness Light Emitting Diodes*, Academic Press, Cambridge, Massachusetts (1997).
7. A. A. Al-Jabr et al., "Large bandgap blueshifts in the InGaP/InAlGaP laser structure using novel strain-induced quantum well intermixing," *J. Appl. Phys.* **119**, 135703 (2016).
8. M. A. Majid et al., "First demonstration of InGaP/InAlGaP based 608 nm orange laser and 583 nm yellow superluminescent diode," in *Photonics Conf. (IPC '15)*, pp. 575–576 (2015).
9. P. Floyd and D. Treat, "Improved performance of laterally oxidized GaInP/AlGaInP lasers by thermal annealing," *Appl. Phys. Lett.* **70**, 2493–2495 (1997).
10. J.-D. Hwang and C.-Y. Lin, "Improving the performance of AlGaInP laser diode by oxide annealing," *Jpn. J. Appl. Phys.* **42**, L1116 (2003).
11. J. Dekker et al., "Annealing of the deep recombination center in GaInP/AlGaInP quantum wells grown by solid-source molecular beam epitaxy," *J. Appl. Phys.* **86**, 3709–3713 (1999).
12. T. Lin et al., "Impurity free vacancy diffusion induced quantum well intermixing based on hafnium dioxide films," *Mater. Sci. Semicond. Process.* **29**, 150–154 (2015).
13. V. Hongpinyo et al., "Intermixing of InGaAs/GaAs quantum well using multiple cycles annealing Cu-doped SiO<sub>2</sub>," in *IEEE Photonics Global@ Singapore*, Singapore, Vol. 404753 (2008).
14. H. S. Djie et al., "Defect annealing of InAs-InAlGaAs quantum-dash-in-asymmetric-well laser," *IEEE Photonics Technol. Lett.* **18**, 2329–2331 (2006).
15. B. S. Ooi, T. K. Ong, and O. Gunawan, "Multiple-wavelength integration in InGaAs-InGaAsP structures using pulsed laser irradiation-induced quantum-well intermixing," *IEEE J. Quantum Electron.* **40**, 481–490 (2004).
16. P. Cusumano et al., "Suppression of quantum well intermixing in GaAs/AlGaAs laser structures using phosphorus-doped SiO<sub>2</sub> encapsulant layer," *J. Appl. Phys.* **81**, 2445–2447 (1997).
17. K. S. Mobarhan, *Test and Characterization of Laser Diodes: Determination of Principal Parameters*, Newport Corporation (1995).

18. A. M. Mohammed et al., "First demonstration of InGaP/InAlGaP based orange laser emitting at 608 nm," *Electron. Lett.* **51**(14), 1102 (2015).
19. A. A. Al-Jabr et al., "Achieving room temperature orange lasing using InGaP/InAlGaP diode laser," in *Advanced Solid State Lasers*, OSA Technical Digest, paper AM5A.46, Optical Society of America, Berlin, Germany (2015).
20. P. Gareso et al., "Influence of SiO<sub>2</sub> and TiO<sub>2</sub> dielectric layers on the atomic intermixing of In<sub>x</sub>Ga<sub>1-x</sub>As/InP quantum well structures," *Semicond. Sci. Technol.* **22**, 988 (2007).
21. O. Kowalski et al., "A universal damage induced technique for quantum well intermixing," *Appl. Phys. Lett.* **72**, 581–583 (1998).
22. B. S. Ooi et al., "Selective quantum-well intermixing in GaAs-AlGaAs structures using impurity-free vacancy diffusion," *IEEE J. Quantum Electron.* **33**, 1784–1793 (1997).

**Ahmad A. Al-Jabr** is a PhD student in the Photonics Laboratory at King Abdullah University for Science and Technology (KAUST), Thuwal, Saudi Arabia. His research is focused on III-V semiconductor lasers. He received his BSc and MSc degrees in electrical engineering from King Fahd University of Petroleum and Minerals (KFUPM), Dhahran, Saudi Arabia. Previously, he served as a lecturer at Jubail Industrial College, Saudi Arabia.

**Pawan Mishra** is currently a PhD student at King Abdullah University for Science and Technology (KAUST), Saudi Arabia, researching into epitaxial growth of III-nitride semiconductors using plasma assisted molecular beam epitaxy. He received his MTech degree in solid state technology from Indian Institute of Technology, Kharagpur, in 2009. He obtained his MSc degree in physics (electronics) and a BSc in physics, chemistry, and mathematics in 2005 and 2003, respectively, from Hemwati Nandan Bahuguna Garhwal University, India.

**Mohammed A. Majid** received his PhD in electronic and electrical engineering from the University of Sheffield, United Kingdom. Currently, he is an assistant professor in the Electrical and Computer Engineering Department, Effat University, Saudi Arabia. Prior to earning his PhD, he worked as a lecturer at KFUPM from 2002 to 2008. His primary research involves experimental work on III-V semiconductor lasers, particularly on quantum dot/well lasers for biomedical imaging, optical communications, and solid state lighting.

**Tien Khee Ng** is currently a senior research scientist at King Abdullah University of Science and Technology (KAUST), Thuwal, Saudi Arabia. His research is centered on semipolar InGaN based laser devices with integrated functionalities, as well as nanowires devices grown on unconventional substrates using plasma assisted molecular beam epitaxy. He is also a coinvestigator for the King Abdulaziz City for Science and Technology (KACST) Technology-Innovation-Center (TIC) for solid-state lighting at KAUST.

**Boon S. Ooi** is a professor of electrical engineering at KAUST. He is also the director of the KACST-Technology Innovation Center (TIC) for solid-state lighting. He received his BEng and PhD degrees in electronics and electrical engineering from the University of Glasgow, Scotland, United Kingdom in 1992 and 1994, respectively. In KSA, major funding support for his research is from King Abdulaziz City for Science and Technology (KACST).